Micro-Hydraulic Structure for High Performance Bio-Mimetic Air Flow Sensor Arrays

Mahdi M. Sadeghi, Rebecca L. Peterson, and Khalil Najafi

Center of Wireless Integrated Micro-Systems (WIMS), EECS Dept., University of Michigan
Ann Arbor, MI, 48109-2122 USA
Tel: +1-734-763-6650, Fax: +1-734-763-9324, E-mail: sadeghi@umich.edu, blpeters@umich.edu, najafi@umich.edu

Abstract

Here we introduce a novel micro-hydraulic structure that can significantly improve performance of many MEMS devices. Using this structure we fabricate and test a new type of low-power, accurate and robust flow sensor in which a hair-like appendage is used to translate flow into hydraulic pressure. This pressure is hydraulically amplified and sensed with a capacitance that is integrated with the micro-hydraulic system. The air flow sensor can detect flow speeds ranging from zero to 10 $m.s^{-1}$ with a resolution of 1 $cm.s^{-1}$ in the low flow regime and a predicted minimum detectable flow of 3 $mm.s^{-1}$.

Introduction

Bio-mimetic hair-like structures can provide air flow sensing with high accuracy and high resolution, and hairs with small footprints enable array fabrication to provide redundancy and fault tolerance. Previous works using hairs with piezoresistive or capacitive transduction have very fragile structures that limit the use of the air sensors in outside environments (1,2). Also, the high accuracy of these sensors is achieved at the expense of dynamic range. Here we exploit a micro-hydraulic structure to overcome these shortcomings. Compared to conventional capacitive air flow sensors (1,6), the sensor based on micro-hydraulic system (3,4) expands the measurement range while maintaining the same sensitivity. In conventional capacitive sensors, a narrow capacitive gap is needed to make the device sensitive to small amounts of plate deflection and thus obtain high sensitivity. However narrow gaps deteriorate the range. In contrast, when hydraulically-assisted capacitive sensing is used, a very large gap can be used on the front side to allow a large range while a narrow back-side gap is used to obtain high sensitivity. A larger capacitive plate area on the back side can compensate for the smaller deflection. In addition, since both gaps are filled with liquid and enclosed, the system is robust and less prone to damage in wet, windy or dusty environments compared to capacitive sensors with exposed gaps or piezoresistive sensors with narrow and fragile cantilever beams. Moreover, capacitive transduction is very low power compared to commonly-used hot wire anemometers (5) or other thermal sensors (6-8).

Device Description

A. Micro-hydraulic system

The basic hydraulic system shown in Fig. 1 consists of two trenches on the front and back side of a silicon wafer connected by a channel. Both trenches and the channel are filled with a silicone fluid and the trenches are capped by a 1-2 μm thick layer of Parylene to enclose the micro-hydraulic system. Each chamber can be compressed by applying

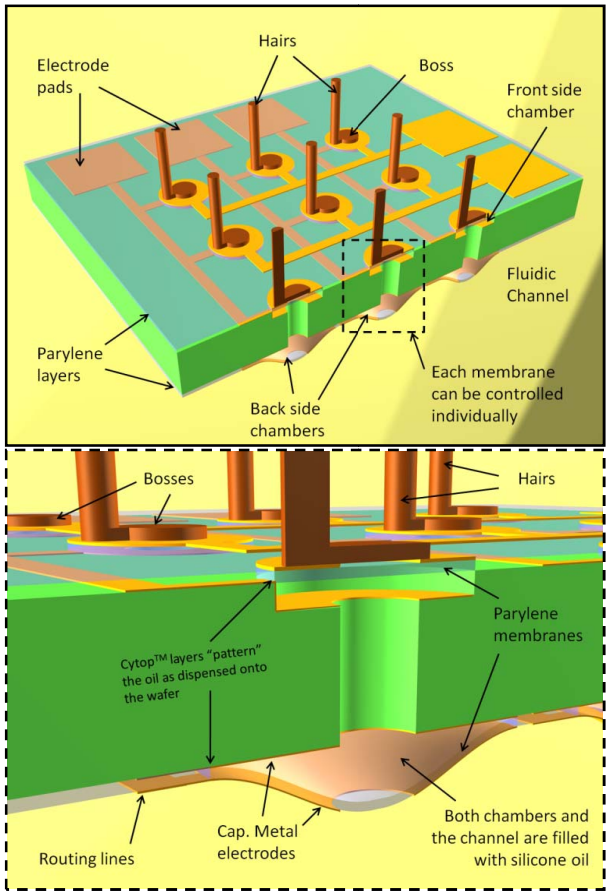

Fig. 1 Micro-hydraulic structure with hairs attached on bossed membrane. The base structure consists of top and bottom chambers and a pair of electrodes on the bottom membrane for either electrostatic actuation or capacitive sensing. After integration of the boss to the system, a silicone elastomer epoxy is used to attach the hair over the boss.

internal or external pressure to the flexible Parylene membrane on one side, thus forcing the liquid into the other chamber, causing its membrane to deflect.

In this hydraulic system, amplification of either force or displacement is achievable with a proper choice of the area ratio between the chambers. This amplification, which is characteristic of the micro-hydraulic system, plays an essential role in improving sensor performance. A pair of electrodes on the back side can be used for electrostatic actuation or capacitive sensing. The fabrication process is shown in Fig. 2.

Fabrication starts with DRIE trenches on the front and back side of the silicon wafer. A stack of evaporated Cr/Au films on the backside forms the first plate of the capacitive sensor. In the next step, Cytop™, which is a hydrophobic polymer, is spun and patterned on both the front and backside of the wafer. This hydrophobic polymer helps to contain liquid droplets in Cytop™-free areas. A channel connecting the back and front-side chambers is made using DRIE. The silicone oil is dispensed and with help of Cytop™ it is contained only in the chambers and channels. Depending on the application, the boss may or may not be included (as described in the following section) and after this the whole structure is encapsulated with Parylene. Since the silicone oil used here (1,3,5-trimethyl-1,1,3,5,5-pentaphenyltrisiloxane) has very low vapor pressure, it is not evaporated during Parylene deposition in a vacuum chamber. For the second plate of the capacitance, Cr/Au is deposited through a shadow mask onto the top of the Parylene layer. An array of micro-hydraulic structures are shown in the Fig. 4 inset.

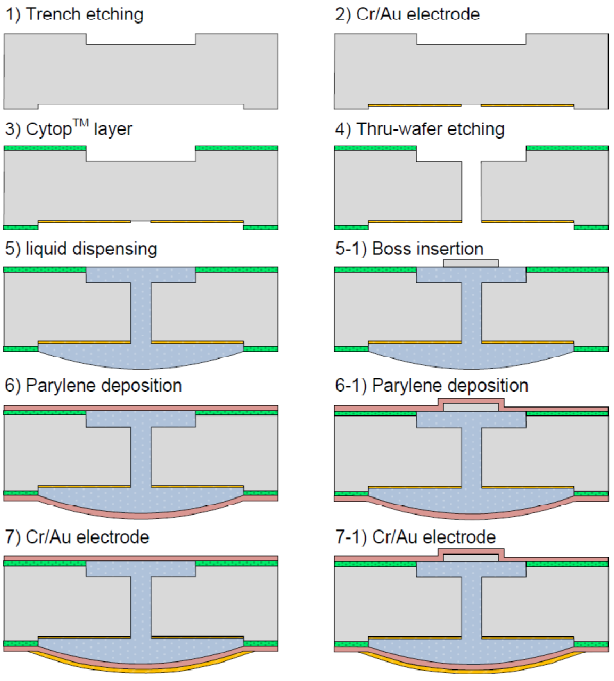

Fig. 2 Fabrication process. Trenches and through-wafer channels are formed by DRIE. Cytop™ is a spin on polymer that makes the surface hydrophobic. Therefore, the fluid will be contained in Cytop™ free areas. In the Parylene deposition step, surface tension keeps the liquid in place. Integration of the boss is shown in process steps 5-1, 6-1 and 7-1.

B. Bossed membrane

To make a hair-like air flow sensor or actuator based on the micro-hydraulic structure, a hair appendage must be attached to the membrane to translate the ambient air flow into hydraulic pressure. A simple process is needed for hair attachment which allows this transduction without altering the rest of the structure. We have developed a technique to integrate a silicon boss as a platform for attaching hair appendages. As shown in Fig. 2 parts 5-1, 6-1 and 7-1, after liquid dispensing, a 100µm-thick silicon disk is put over the fluid and Parylene is deposited. The disk does not sink and is aligned in the center due to surface tension (Fig. 3,4). After boss integration, a pre-fabricated pin can be attached to the boss in a minimally invasive way without excessive adhesive/paste reflow or residues which might alter the Parylene membrane mechanical properties (Fig. 5). We have successfully tested an air flow sensor made by attachment of a hair on a bossed membrane. The bossed device obtains the same performance as an un-bossed device while scaling down the device geometry by 2.5× in hair length and 4× in capacitance area.

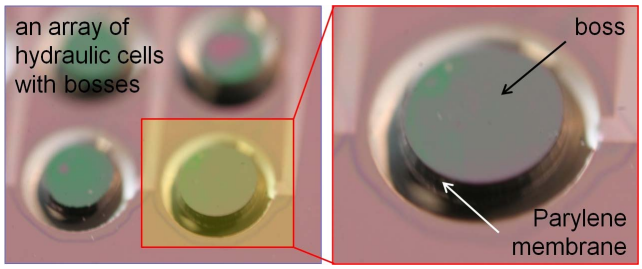

Fig.3 An array of micro-hydraulic cells with bossed top membranes. As shown in the figure, the boss does not sink into the fluid and is self-aligned in the center.

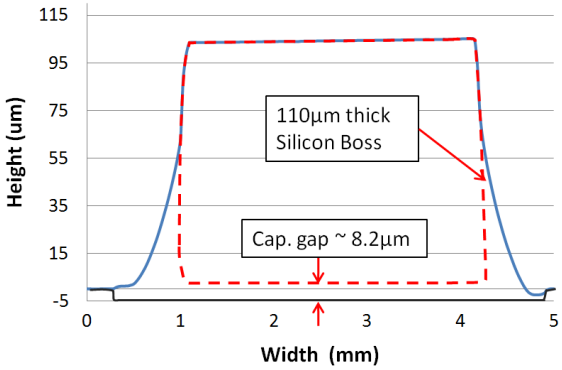

Fig.4 Surface profile of one cell with bossed membrane over a 4.5 µm trench. As shown in the image the boss is aligned in the center and it rests in a fairly flat position.

C. Hair sensor

To produce an air flow sensor based on the micro-hydraulic system, a hair-like post that extends from the surface out of the plane of the substrate is needed to convert a fluid drag force into pressure and to exert pressure on the boss and thus on the front-side membrane. The boss pushes the liquid toward the back side, deflecting the back-side membrane. A pair of metal electrodes is deposited on the back-side Parylene membrane and on the substrate underneath to form a capacitor. As flow speed increases, the membrane deflects, and the capacitance decreases monotonically. Since the capacitive gap is enclosed, this sensor is more robust compared to structures which locate the hair over a narrow cantilever beam or on top of an exposed, narrow-gap capacitive plate. Fig. 5 shows a micro-hydraulic hair sensor. The boss under the pre-fabricated pin can be clearly seen.

The fabricated devices have been tested in a wind-tunnel. The sensors are placed in the laminar flow region of the tunnel. The air flow speed is monitored with a commercial hotwire anemometer located next to the sample while the capacitance change is measured with a HP 4284A LCR meter. Fig. 6 shows measured capacitance change versus air flow speed. The sensor operates over a wide range up to 10 $m{\cdot}s^{-1}$. Five different sensors were fabricated and measured. The low flow sensitivity was found to range from 230 to 440 $fF/(m{\cdot}s^{-1})$, with an average of 333 $fF/(m{\cdot}s^{-1})$. For the device shown in Fig. 6, the low flow sensitivity is 315 $fF/(m{\cdot}s^{-1})$. Therefore if the capacitive readout circuit can detect a capacitance change of 1 fF, the minimum detectable flow is ~3 $mm{\cdot}s^{-1}$.

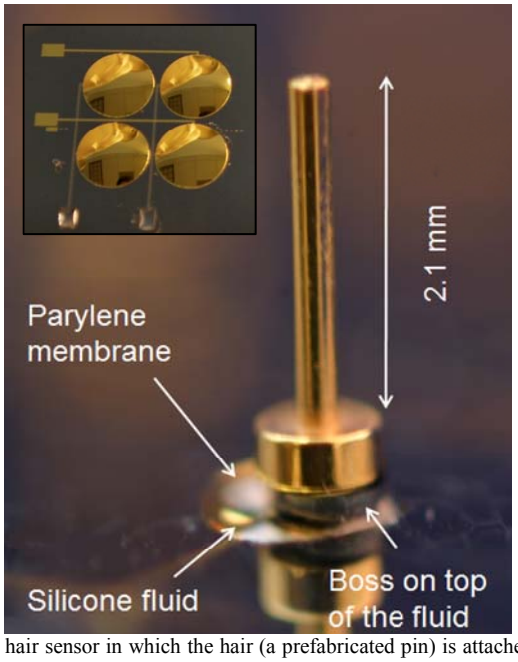

Fig. 5 A hair sensor in which the hair (a prefabricated pin) is attached to the front-side membrane over the boss. On the top left, the back side of an array of four cells is shown.

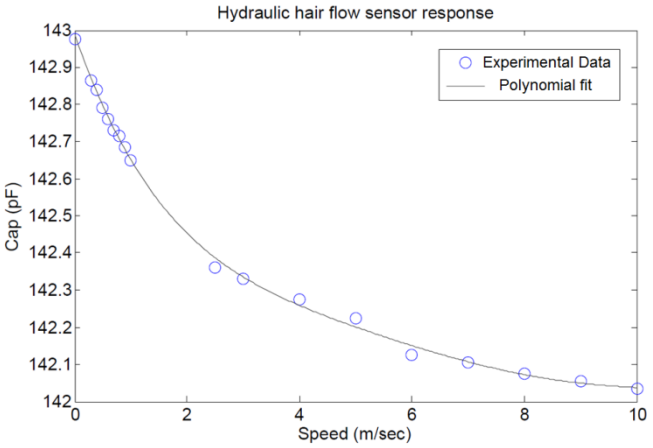

Fig. 6 Micro-hydraulic air flow sensor response to air flow speed. In the low flow region (for 0-1 $m{\cdot}s^{-1}$) the capacitive rate of change is 315fF/$m{\cdot}s^{-1}$. The data fit line is a 5th-degree polynomial. The variation of measured data from the fit line is used to determine the 1 $cm{\cdot}s^{-1}$ resolution of the sensor.

D. Simulation

To verify the experimental results, we used the structural mechanics component in the MEMS module of COMSOL to model the micro-hydraulic hair air flow sensor. The dimensions of the fabricated device characterized in Fig. 5 were used in the model (Table I). The simulated membrane and hair structure are shown in Fig. 7. For a given air flow, the resultant drag force on the hair is calculated analytically. This force is then applied to the hair tip in COMSOL, which predicts the resultant deflection of the tip and the 3-D membrane displacement. From the displacement, the volume change under the front-side membrane is calculated. Assuming the silicone oil is an incompressible fluid such that the entire liquid volume change is transferred to the back-side, the back-side membrane deflection is calculated. Using the capacitance-gap relation of a curved electrode capacitor, the expected change in back-side capacitance is determined. The back-side curved electrode geometry and the equations used to calculate the volume and capacitance between the curved electrode and the flat electrode are given in Table II. Note that these equations assume that the height of the liquid droplet is much smaller than its diameter.

TABLE I
DIMENSIONS OF FABRICATED DEVICE

Parameter	Value
Parylene membrane thickness	1 µm
Parylene membrane diameter (Front)	1 mm
Parylene membrane diameter (Back)	2.24 mm
Hair height	1.9 mm
Hair diameter	220 µm
Boss thickness	118 µm
Boss diameter	474 µm
Front side recess depth	4.5 µm
Back side recess depth	2 µm

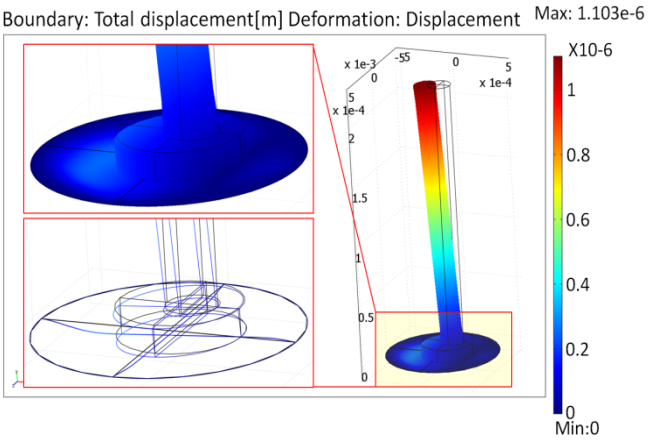

Fig. 7 Simulation result of a hair deflected in response to air flow with a speed of 1 m·s^{-1} (*i.e.*, a drag force of 0.157 µN is applied to the hair tip.) The radial displacement is plotted at 128.5x its actual value, for visibility.

TABLE II
GEOMETRY AND FORMULAS USED TO CALCULATE THE CAPACITANCE CHANGE ON THE BACKSIDE OF THE AIR FLOW SENSOR

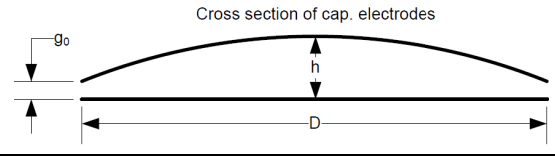

Volume $$\pi\left(\frac{D^2+4h^2}{D^2}\right)\times\left[\frac{1}{3}\left(\frac{D^2-4h^2}{D^2+4h^2}\right)^3-\left(\frac{D^2-4h^2}{D^2+4h^2}\right)+\frac{2}{3}\right]$$

$$if\ D \gg h \rightarrow Volume \cong \frac{\pi}{8}hD^2$$

Capacitance $$\pi\varepsilon\frac{D^2+4h^2}{4h}ln\left(\frac{g_0+h}{g_0}\right)$$

For the geometry of the device characterized in Fig. 6, simulation predicts that at 1 m·s^{-1} of air flow (or 0.157 µN at the hair tip), the tip of the hair appendage will be deflected by 1.103 µm. This deflection is shown on the right in Fig. 6, where the radial deflection is amplified in the plot by a factor of 128.5 in order to make it visible. This causes a front-side membrane deflection of 300 nm and a volume change of 6.28×10^{-14} m^3 under the front-side membrane. This corresponds to a predicted back-side maximum membrane deflection of 32 nm resulting in a capacitance change of 150 fF. This is of the same order of magnitude as the measured result of 230 fF capacitance change for 1 m·s^{-1}. Differences between the experimental and simulation results may come from ambiguity in calculations of the fluid drag force and drag coefficient at very low flow speeds (i.e., at low Reynolds' number as seen in (1,2)), and from non-idealities of the fabricated device, including slight curving of the front side membrane. Note the ~10x hydraulic amplification ratio between the front-side and back-side membrane deflection (300 nm vs 32 nm.) Table III summarizes the results.

TABLE III
SUMMARY OF RESULTS FOR 1 m·s^{-1} AIR FLOW

Simulation results and experimental data	
Maximum deflection of the front side membrane	300 nm
Liquid volume transfer	6.28×10^{-14} m^3
Maximum deflection of the backside membrane	32 nm
Backside capacitance change (Modeling)	150 fF
Backside capacitance change (Measured)	230 fF

Conclusions

We have introduced a novel hair-like air flow sensor based on a micro-hydraulic structure. The hair sensor is successfully fabricated and tested and offers a large measurement range while maintaining high sensitivity. Simulation and experimental results are in reasonable agreement. The micro-hydraulic system can be used as a new design element in a variety of MEMS devices to improve their performance.

Acknowledgments

The authors thank Michael T. Chaney for his help in testing and characterization of the device, and the staff of the Lurie Nano-fabrication Facility (LNF), a member of the National Nanotechnology Infrastructure Network, which is supported in part by the National Science Foundation, for their help in device fabrication. This project is funded by the MAST Program of the Army Research Lab (ARL) under Award Number W911NF-08-2-0004.

References

(1) C. M. Bruinink, *et al.*, "Advancements in technology and design of biomimetic flow-sensor Arrays," *IEEE Int. Conf. on Microelectromechanical Systems (MEMS), Sorrento, Italy*, pp. 152-155, January 2009.

(2) N. Chen, C. Tucker, J.M. Engel, Y. Yang; S. Pandya, C. Liu, "Design and characterization of artificial haircell sensor for flow sensing with ultrahigh velocity and angular sensitivity," *J. Microelectromech. Syst. (JMEMS)*, vol. 16, pp. 999-1014, October 2007.

(3) H. Kim, K. Najafi, "An electrically-driven, large-deflection, high-force, micro piston hydraulic actuator array for large-scale micro-fluidic systems," *IEEE Int. Conf. on Microelectromechanical Systems (MEMS), Sorrento, Italy*, pp. 483-486, January 2009.

(4) M. Sadeghi, H. Kim and K. Najafi, "Electrostatically driven micro-hydraulic actuator arrays," *IEEE Int. Con. on Microelectromechanical Systems (MEMS), Hong Kong, China*, pp. 15-18, January 2010.

(5) M. Sadeghi, R. L. Peterson, K. Peterson, R. Fearing and K. Najafi, "Air-flow sensing on autonomous mobile platforms using micro-scale hot-wire anemometry," *27th Army Science Conference, Orlando, FL*, December 2010.

(6) Y. H. Wang, *et al.*, "MEMS-based gas flow sensors," *Journal of Microfluidics and Nanofluidics*, vol. 6, pp. 333-346, March 2009.

(7) G. Kaltsas, A. G. Nassiopoulou, "Novel C-MOS compatible monolithic silicon gas flow sensor with porous silicon thermal isolation," *Sensors and Actuators A: Physical*, vol. 76, pp. 133-138, August 1999.

(8) R. Buchner, C. Sosna, M. Maiwald, W. Benecke, W. Lang, "A high-temperature thermopile fabrication process for thermal flow sensors," *Sensors and Actuators A: Physical*, vol. 130-131, pp. 262-266, August 2006.